

## Narrow Components in the Angular Correlation of Annihilation Quanta from Condensed Materials\*

LORNE A. PAGE AND MILTON HEINBERG  
*University of Pittsburgh, Pittsburgh, Pennsylvania*

(Received January 23, 1956)

Measurements on the angular correlation of two-photon annihilation of positrons within 10 milliradians of  $180^\circ$  show that amorphous materials, known or expected to have a long-lived component, have a more pointed distribution than crystalline materials, as though a narrow component were present. The former group includes fused quartz, Teflon, polystyrene, polyethylene, paraffin, Lucite, and glass; the latter, crystalline quartz, aluminum, magnesium, copper, graphite, and sulfur crystals. Cane sugar, either as "crystals" or as a plastic material, is empirically classified with the narrow-component group. Magnetic experiments up to 16.3 kilogauss cause a transfer of 3 to 4% of the annihilation events into the narrow component from the rest of the events, when the narrow component already exists in the material in agreement with the assumption that a triplet state of a positron-electron system is being quenched. Experiments under way are designed to estimate the positron-electron overlap by measurement of the field dependence of this effect. A preliminary experiment on possible diffusion of annihilation centers is described.

### I. INTRODUCTION

THIS paper describes a number of positron annihilation experiments done in this laboratory over the past year. The experiments deal with the angular correlation of two-photon events<sup>1</sup> occurring when positive beta rays are directed into samples of various condensed materials. Generally the angle was limited to within 10 milliradians of  $180^\circ$  paying particular attention to the narrow component, which was first observed in a fused quartz annihilator.<sup>2</sup>

The experiments are designed to show whether the narrow component, when present, behaves in a manner consistent with the hypothesis that positronium, or something like it, is formed in certain condensed materials.<sup>3-5</sup> Thus contact is sought with the positron lifetime results of Bell and Graham<sup>3</sup> by using some of the same annihilating materials as these authors. Because of the possible connection between  $^3S$  states of positronium and the narrow component, an enhancement of this component by a strong magnetic field was looked for. The magnetic quenching experiments<sup>6-8</sup> done in various gases, serve as a guide for quenching experiments in condensed materials, except that here one studies the magnetic sensitivity of the narrow components, rather than the magnetic sensitivity of the three- or two-quantum yields.<sup>9</sup> Although brief

reports have already been given of a part of the work,<sup>2,10</sup> all results to date are collected here for completeness, including some preparatory work on possible diffusion of annihilation centers.

### II. EXPERIMENTS

#### (1) Angular Correlation in Quartz

##### (i) Apparatus

Figure 1 shows, not to scale, the apparatus used for the quartz experiment and certain of the later experiments. Reading from left to right in Fig. 1(a) one has: a NaI(Tl) scintillator,  $1\frac{1}{4} \times 1\frac{1}{4} \times \frac{1}{4}$  inches, designated *A*; adjacent to this, a pair of lead bricks forming a detector slit of adjustable width; a pair of lead bricks forming a defining slit adjacent to the source-sample assembly, which is located at the center of the apparatus (designated *O*) and a similar slit system for detector *B*. All items to the right of *O*, *viz.*, defining slit, detector slit, and the second scintillator, *B*, are carried as a rigid unit on an arm pivoted about an axis normal to the page through *O*. An enlarged sketch of the source-sample assembly is shown in Fig. 1(b). The active material (5 mC of  $\text{Na}^{22}$ ) is spread over a stainless steel disk 0.8 inch in diameter. A mechanical vacuum is maintained between source and sample. The annihilating sample is a disk with a one-inch diameter well whose depth is 0.156 inch. With defining slits set at 0.030 inch, angle  $\theta$  set at zero, it is a simple matter to isolate two-photon events in the sample from events in the source itself, by observing coincidence rate between scintillators *A*, *B* as the source-sample unit is moved by means of a screw feed along its own (vertical) axis; see typical curve, Fig. 1(c), (in this case a polystyrene sample). Perhaps 20% of the total positrons end up in the sample.

\* Work done in the Sarah Mellon Scaife Radiation Laboratory and sponsored by the Office of Ordnance Research, U. S. Army.

<sup>1</sup> DeBenedetti, Cowan, Konnecker, and Primakoff, *Phys. Rev.* **77**, 205 (1950).

<sup>2</sup> Page, Heinberg, Wallace, and Trout, *Phys. Rev.* **98**, 206 (1955).

<sup>3</sup> R. E. Bell and R. L. Graham, *Phys. Rev.* **90**, 644 (1953).

<sup>4</sup> M. Deutsch, *Progr. Nuclear Phys.* **3**, 131 (1953).

<sup>5</sup> S. DeBenedetti and H. C. Corben, *Ann. Rev. Nuclear Sci.* **4**, 191 (1954).

<sup>6</sup> M. Deutsch and E. Dulit, *Phys. Rev.* **84**, 601 (1951).

<sup>7</sup> T. A. Pond and R. H. Dicke, *Phys. Rev.* **85**, 489 (1952).

<sup>8</sup> J. Wheatley and D. Halliday, *Phys. Rev.* **88**, 424 (1952).

<sup>9</sup> Compare also T. A. Pond, *Phys. Rev.* **93**, 478 (1954), and R. L. Graham and A. T. Stewart, *Can. J. Phys.*, **32**, 678 (1954).

<sup>10</sup> Page, Heinberg, Wallace, and Trout, *Phys. Rev.* **99**, 665(A) (1955); and Army Ordnance Technical Report, University of Pittsburgh (unpublished).

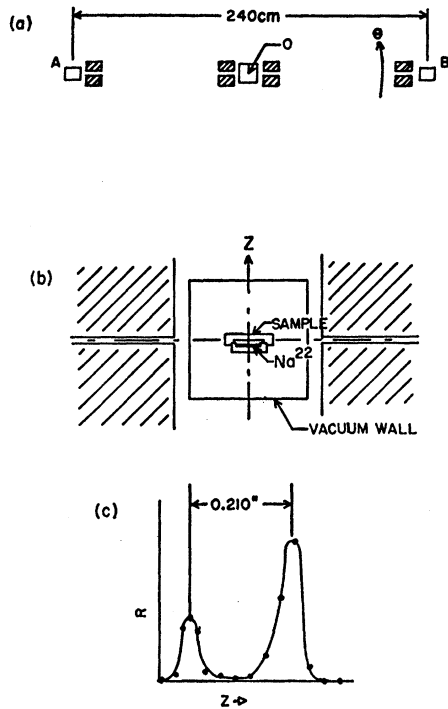


FIG. 1. (a) Elevation view of apparatus; (b) enlarged view of source-sample assembly; and (c) curve of coincidence rate,  $R$ , versus elevation of source-sample assembly,  $z$ .

The coincidence circuit employs a pair of crystal diodes, followed by a pulse-stretcher. DuMont 6292 photomultipliers are used, and each collector feeds two Hewlett Packard Model 460A wide-band amplifiers in series. Normally 15-foot shorted stubs are used on the outputs, giving adequate signal-to-noise ratios without undue loss of pulse height. For a time, single-channel discriminators in coincidence with the "fast" coincidence output were employed on the individual signals from the last dynodes of the photomultipliers; however, no noticeable improvement in stability or in signal-to-noise ratio was found to justify this refinement, and its use was discontinued.<sup>11</sup> During data-taking, the high voltages for the photomultipliers and the individual  $B$ -voltages of the wide-band amplifiers are monitored several times per hour. The signal from the coincidence circuit feeds two independent linear amplifiers and in turn two independent discriminator-scaler units.

### (ii) Results

Geometrically identical fused and crystal quartz samples were compared first as regards to relative width at half-maximum with moderate angular resolution,  $\Delta\theta=5$  milliradians. That is, each detector subtends  $\Delta\theta$  at the center. The result was that the fused quartz curve,  $F$ , was narrower than the crystalline quartz

<sup>11</sup> The chance of a 1.3-Mev nuclear gamma ray being counted in coincidence with a 0.5- or a 1.3-Mev gamma should of course be small in view of the geometry.

curve,  $C$ , as shown in Fig. 2(a), where both angular correlation curves are plotted with the same area. On narrowing the resolution to  $\Delta\theta=0.8$  milliradian, the data, Fig. 2(d), show the fused and crystalline quartz curves to be quite different in shape. Here, as throughout the paper, the uncertainties shown are standard deviations based on the number of counts. In this plot, the relative normalization is chosen for best fit for  $\theta$  beyond the half-value points of the  $C$ -curve. The difference,  $(F-C)/C_{\max}$ , denoted by  $\gamma$ , derived from curves (d) is plotted as curve (e) in Fig. 2. The area under curve (e) corresponds to about 20% of the area of the parent curve  $F$ . No reasonable fitting in the wings would change this estimate to anything as high as 29%—the fraction of positrons in the long-lived component.<sup>3</sup> Fused and crystalline quartz were also run at an intermediate  $\Delta\theta$  of 2.5 milliradians, and the difference curve only is plotted in Fig. 2(c).

It was thought advisable to try for a better number for the fraction appearing in the narrow component. Accordingly, with  $\Delta\theta$  set at 5 milliradians in the interest of high counting rate (about 15 coincidences per second), extensive data were taken as follows: at each  $\theta$  to be run, an empirical integration<sup>12</sup> was made by moving detector  $A$  in half-inch steps parallel to the  $x$ -axis, normal to the page in Fig. 1(a). These data represent what would happen for a short line segment source, one similar detector, and one infinitely long

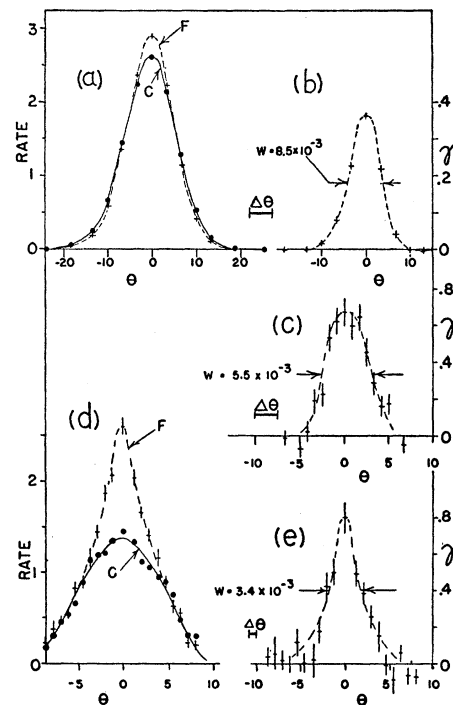


FIG. 2. Angular correlation for fused quartz,  $F$ , and crystalline quartz,  $C$ . Angle  $\theta$  is in milliradians.

<sup>12</sup> Actually a  $\theta$  curve was run at each  $x$ -setting needed, which was mechanically easier to do.

detector. The total counts under  $F$  then agree within 2% with those under  $C$  when correction has been made for the measured difference in gamma ray absorption of these two samples. No attempt was made here to repeat the work of Pond on two-quantum yields.<sup>9</sup> The points of Fig. 2(a) each involve about  $3 \times 10^4$  counts near the peak and proportionately fewer in the wings. Background was taken to be coincidence rate at  $\theta = \pm 27$  milliradians; for  $x=0$ , (peak rate)/(background rate) was 200:1. Curves  $F$  and  $C$  are then renormalized for "best fit" in the wings of the curve, i.e., beyond  $\sim 10$  milliradians from the center, and the derived difference  $\gamma$ , defined as above, is plotted as curve (b). Its area is equivalent to 0.18 of the parent  $F$  curve. The uncertainty in the choice of renormalization was thought to be  $\sim 3\%$ , which implies an uncertainty in the figure 0.18 of at most 15% of itself.

The foregoing has been a description of the quartz work done prior to the original publication.<sup>2</sup>

It should be mentioned that the optic axis of the crystalline quartz sample was in the  $z$ -direction (see Fig. 1), and projected angles were measured always with respect to a plane normal to this direction. However, some graphite data had previously been taken ( $\Delta\theta = 5$  milliradians) on the half-width of the angular correlation, comparing two samples cut from a large natural crystal. No difference was found, to within 0.2%, between basal planes normal to  $z$  and basal planes parallel to  $z$ . It was assumed then, that with crystalline quartz, at the same resolution, the angular correlation would be reasonably independent of crystal orientation in the apparatus, and thus a favored orientation had not accidentally been chosen in the above quartz experiment.

## (2) Classification of Annihilating Materials

An immediate extension of the quartz experiment was to see whether amorphous materials in general have a pointed angular correlation like fused quartz, in contrast to crystalline materials. A Teflon sample was run first in the apparatus described above, with

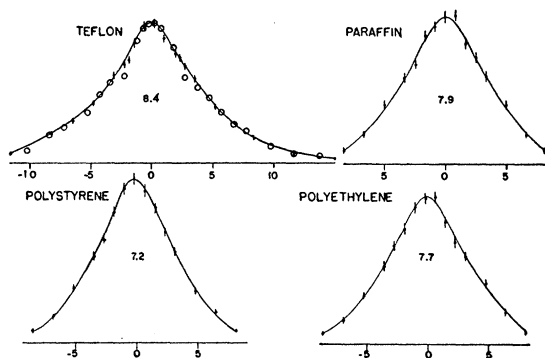


FIG. 3. Angular correlation for four amorphous materials with  $\Delta\theta = 0.8$  milliradian. Abscissas are milliradians. Angular half-widths are indicated. The circles on the Teflon curve are the data of Lang and DeBenedetti.

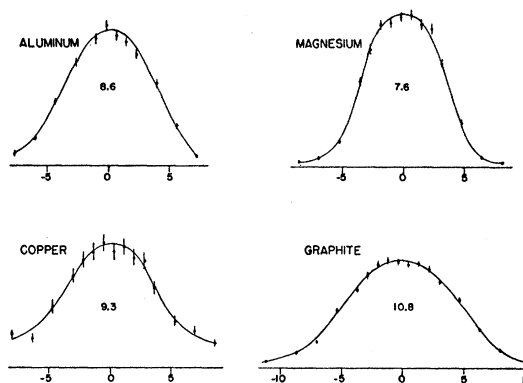


FIG. 4. Angular correlation for four crystalline materials with  $\Delta\theta = 0.8$  milliradian. Angular half-widths in milliradians are indicated.

$\Delta\theta = 0.8$  milliradian. As already stated,<sup>2</sup> the result was similar to that for fused quartz. Figure 3 shows the angular correlation for Teflon,<sup>13</sup> and for three other amorphous materials, all run with  $\Delta\theta = 0.8$  milliradian. It is noted that these materials (save paraffin) are known to exhibit a long-lived component.<sup>3</sup> The points of inflection for each curve of Fig. 3 are seen to lie noticeably above the half-value points. Teflon data have since been reported by Stewart.<sup>14</sup>

For comparison, some crystalline materials were run and the curves, Fig. 4, are considerably blunter than the curves for the amorphous materials just discussed. The points of inflection now occur at or somewhat below the half-value points.

In order to emphasize the pointedness associated with the amorphous materials, it was decided to fit each angular correlation curve to the aluminum curve, arbitrarily taken as the standard. This has been done in Figs. 5 and 6. For each material, the rate has been renormalized and the *scale of  $\theta$  altered* so as to fit the dashed aluminum curve at three points: the peak and the two points at 0.25 of peak height. A measure of pointedness for a given material can be had by comparing the width of the modified curve at 0.80 of peak height with this width for aluminum (see upper arrows on the fused quartz curve in Fig. 5). This figure of pointedness,  $f$ , is noted on each of the curves in Figs. 5 and 6. Of these materials, four are blunt with  $f$  approximately unity, and six are definitely more pointed, with  $f$  about 0.6.<sup>15</sup> Sulfur crystals, not shown,

<sup>13</sup> The present Teflon data and those taken by G. Lang and S. DeBenedetti (the circles of Fig. 3) at Carnegie Institute of Technology using the same resolution, are seen to be in agreement. We are grateful for their permission to include their unpublished results here.

<sup>14</sup> A. T. Stewart, Phys. Rev. **99**, 594 (1955).

<sup>15</sup> In Fig. 6 we note that  $f$  is somewhat less than unity for copper (the only "heavy" metal run here) due to its pronounced wings, while the figure is somewhat greater than unity for magnesium corresponding to its lack of wings. See the thorough study of metals by Lang, DeBenedetti, and Smoluchowski, Phys. Rev. **99**, 596 (1955); see also A. T. Stewart.<sup>14</sup> Thus we say that copper does not have a narrow component, but that it does have broad wings.

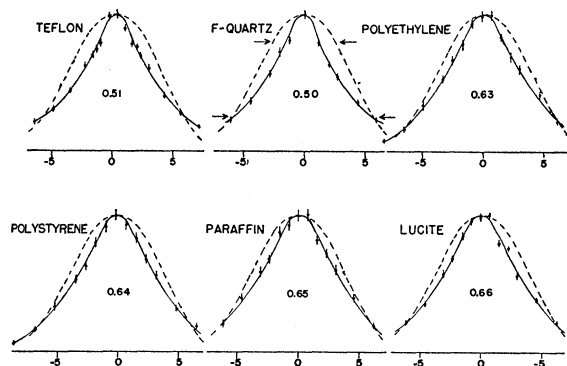


FIG. 5. Angular correlations for six amorphous materials, each adjusted to fit the dashed aluminum curve at the peak and at 0.25 of peak height. The abscissa is milliradians of  $\theta$  for aluminum. The figure of pointedness,  $f$ , is indicated for each material.

have an  $f$  of 0.94. Incidentally, a triangle would have  $f=0.57$ .

Figure 7 shows two more materials that have been surveyed. Part (a) represents cane sugar prepared by melting and cooling to room temperature to form a plastic material. Its figure of pointedness,  $f$ , is 0.70, classifying it with the pointed materials of Fig. 4 rather than the blunt materials of Fig. 5. Part (b) of Fig. 7 shows another sample of cane sugar, prepared by slow (6 weeks) evaporation of a thick solution in water, the resulting mass being then machined; here,  $f=0.71$ . The half-widths for the two sugar samples were respectively 9.4 and 8.2 milliradians. Geometrically, the plastic sample was the cleaner, being denser, and having a flatter surface. Therefore the difference is probably real, but has not been double-checked experimentally. The crystalline cane sugar is classified with the pointed materials but represents the only "crystal" tested which is made up of large molecules.<sup>16</sup>

Finally, a glass lens with a flat surface was run, and the result is plotted in Fig. 7(c);  $f$  turns out to be 0.64. Intensive data were then taken on this sample

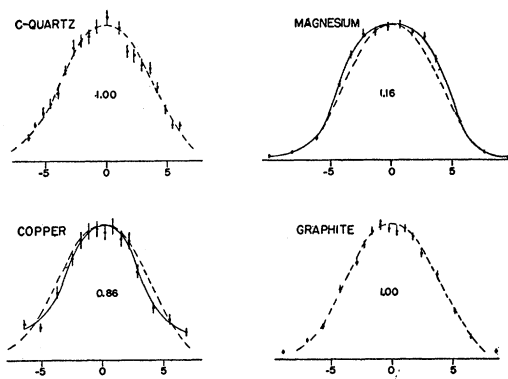


FIG. 6. Angular correlations for four crystalline materials, each adjusted to fit aluminum; see caption for previous figure.

<sup>16</sup> Recent comments along these lines have been made by P. R. Wallace, Phys. Rev. **100**, 738 (1955).

in the vicinity of the peak, with resolution now set at  $\Delta\theta=0.6$  instead of 0.8 milliradian to see whether or not real "shoulders" would appear close to the peak. The result is plotted as Fig. 7(d), and there is only a vague suggestion of shoulders. No doubt it would be better, in looking for shoulders, to try to measure true angles rather than projected angles as is done here.

To sum up in terms of the long-lived component, there has been no contradiction of the rule that when the  $\tau_2$  component is present, a narrow component likewise is present, and when it is not, one has a blunt angular correlation.

### (3) Magnetic Quenching Experiments

Since the estimated fraction of narrow-component (for fused quartz at least), namely about 20%, seems to be significantly smaller than Bell and Graham's 29% fraction of long-lived component, it is interesting to test whether the narrow component can be enhanced by a strong magnetic field. Apparently a fair fraction of the  $^3S$  states (which one might guess provide some, or perhaps all, of the narrow component) do not end up in the narrow component due to moderately violent collisions. Thus it is tempting to try to divert some of these states from a violent end by means of the triplet-singlet conversion demonstrated in the past for gases.<sup>6-8</sup> Here the conversion time must be comparable to the rather short lifetime,  $\tau_2$  of the order of  $10^{-9}$  sec, and so one should use a stronger magnetic field than in the gas experiments.

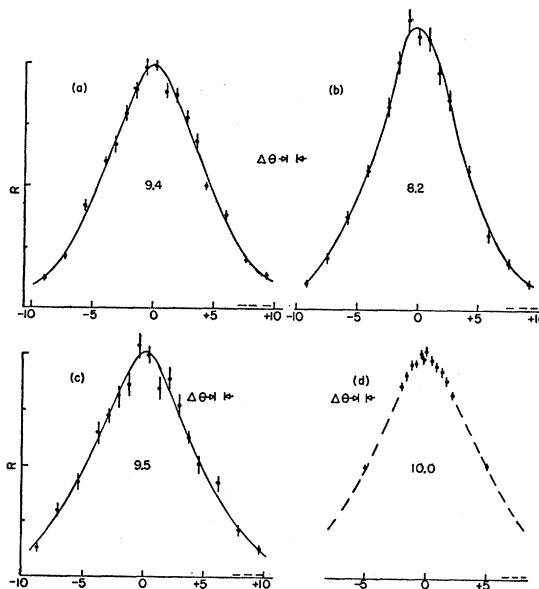


FIG. 7. Angular correlation (a) for "plastic" cane sugar, (b) for cane sugar "crystals", and (c) for a glass sample run at  $\Delta\theta=0.8$  milliradian. Curve (d) represents the same glass sample re-run with  $\Delta\theta=0.6$  milliradian. Angular half-widths are indicated. The dashed lines at the bottom of each figure is the background rate.

Again, for materials exhibiting no sign of a narrow component and no long-lived component, one might expect the angular correlation to be independent of magnetic field. As will be seen, this is the result obtained, which is interpreted as a test of the apparatus for systematic errors (mechanical, thermal, magnetic) introduced by the electromagnet whose field has to be varied.

For these experiments, the apparatus was modified as indicated in Fig. 8(a), where the source-sample assembly is sketched. The source mount was recessed slightly into the lower pole piece of an electromagnet. Annihilating samples of the same inner diameter as in sub-sections (1) and (2) were used, but the well depth was changed to 0.100 inch. Rigid samples could serve as their own vacuum wall, while plastic samples were encased in an aluminum vacuum housing (not shown) to avoid deformation. Lead pads were laid adjacent to the sample, as shown, to mask off essentially all of the annihilation radiation from the cylindrical inner wall of the sample so as to avoid a shift of the angular correlation curve occurring because the magnetic field changes the positron intensity distribution over the surface of the sample, the so-called focusing effect. Alignment procedure was to first align optically the two detector slits, two defining slits, and the axis of rotation for  $\theta$ ; with sample inserted, the electromagnet as a whole was then run up and down in steps of a few by 0.001 inch to achieve maximum coincidence rate from the sample.

It was first ascertained that the half-width for a fused quartz sample narrowed about 10% when 16 kilogauss was applied, and that the half-width for crystal quartz was unchanged at this field value.

Next, a Teflon sample was run at  $\Delta\theta=1.5$  milliradians, and the resulting angular correlation is shown in Fig. 9(a). At each angle  $\theta$  of interest, coincidence rate was measured with the 16-kilogauss field on and with the field off (magnetically cycled to "zero" residual field), without changing the angle. Many sweeps in angle were made in this fashion. The magnet poles were water-cooled so that no systematic temperature variation could affect the sample. Furthermore,

FIG. 8. (a) Source-sample assembly modified for early magnetic experiments and (b) mercury pool added to lower pole piece for later magnetic and diffusion experiments.

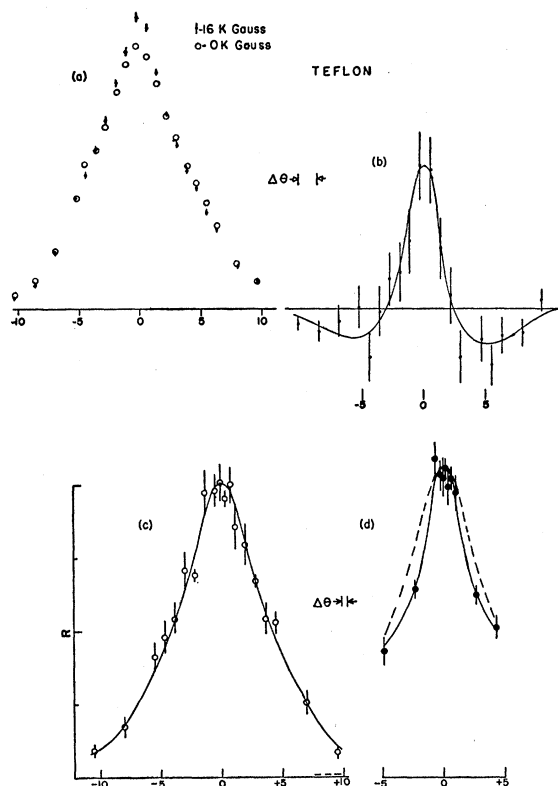
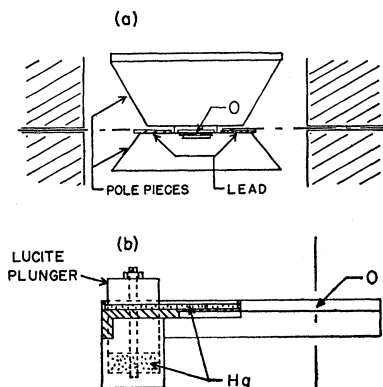


FIG. 9. Teflon quenching data. Points (a) are angular correlation at 16 and 0 kilogauss. The points in (b), derived directly from (a) by subtraction, give a difference curve. Slit width  $\Delta\theta$  was 1.5 milliradians. Curve (c) is angular correlation with  $\Delta\theta$  of 0.42 milliradian, at zero field. Points (d) were run with the same slit width at 16 kilogauss. The dashed curve is renormalized curve (c).

it is believed that no change in resolution could arise systematically.<sup>17</sup>

For the data of Fig. 9(a), peak-to-background exceeded 200:1. Difference points, representing 16-kilogauss data minus 0-kilogauss data, are shown in Fig. 9(b). Evidently a transfer,  $(4.2 \pm 0.5)\%$  of the total annihilations, has been effected from the wings of the distribution into the narrow component, as reported earlier.<sup>10</sup> Thus a quenching effect has been demonstrated. The fact that the Teflon difference

<sup>17</sup> To be sure, the focusing effect does bring in a somewhat larger percentage of the lesser penetrating positrons [discussed in Sec. II (2)], making the effective vertical width of the gamma ray source somewhat less with the field on; however, we are sure this is too small to alter the results presently under discussion. Regarding systematic magnetic interaction with the photomultipliers, test data were taken on the coincidence rate and on the integral-discriminator counts (singles) from one or other of the photomultipliers. With no magnetic shielding on the photomultipliers, the singles rate dropped 20% from field off to maximum field. With standard mu-metal shields on, the singles rate changed at most 0.1 of what it had previously. The addition of the mu-metal shields had no apparent effect on the coincidence rate, the difference being  $(0.7 \pm 3.4)\%$ . All magnetic experiments were run with the shields on. No fluctuation in the ac line voltage or any of the other monitored voltages could be traced to operation of the electromagnet.

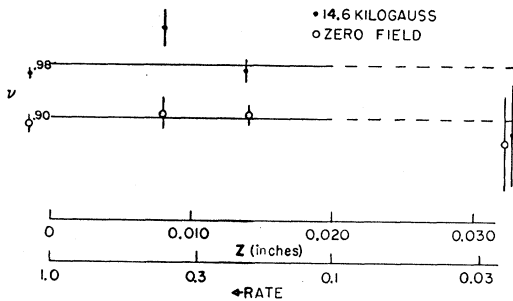


FIG. 10. Narrowness,  $\nu$ , for polyethylene as a function of depth in the sample,  $z$ . Approximate relative coincidence rate is shown along the abscissa.

curve had a net positive area is interpreted as due to the focusing effects.

Teflon was next run with  $\Delta\theta$  narrowed to 0.42 milliradian. With no field, the angular correlation was that of Fig. 9(c). A partial curve was run at 16 kilogauss, with emphasis on angles close to zero, Fig. 9(d). Here comparison is made by vertical renormalization of the zero-field curve to match the peak rate for the 16-kilogauss curve, as indicated in the figure. The narrowing on application of the field is evident. The peak rate was 30 coincidences per kilosecond, and background (at  $\theta=20$  milliradians) was 150 times smaller.

To date, no complete curve with good statistics has been run for fused quartz with the field on. However, intensity data has been taken at three angles, corresponding to the peak and to  $\pm 5.0$  milliradians on either side of the peak, with the field alternately off and on. The ratio of the peak rate to the sum of the other two rates for each field setting, called  $\nu$ , is taken as a measure of narrowness. Because of the symmetry of the angular correlation curve about  $\theta=0$ ,  $\nu$  is insensitive in first order to any systematic shift<sup>18</sup> in the angle  $\theta$  when the field is applied. Some 250 hours of essentially continuous running gave  $\nu$  (16.3 kilogauss) =  $1.543 \pm 0.007$ , and  $\nu(0 \text{ field}) = 1.399 \pm 0.007$ . Each  $\nu$  value here has been corrected for measured background, which is not sensibly different from field off to field on. Allowing for background increases each  $\nu$  by 0.5%. During the 300 measurements of  $\nu$  made for each field setting, the quenching effect was consistent.<sup>19</sup>

<sup>18</sup> No such shift has been apparent when the lead pads of Fig. 8(a) are properly in place, and all quenching data has been taken in this manner. Only the left-hand pad is set critically; the pad on the right is relaxed (about 0.010 inch) to allow for varying the angle  $\theta$ .

<sup>19</sup> The quartz samples are of optical grade, precision ground, and were obtained from the Unertl Optical Company, Pittsburgh, Pennsylvania. In the early work, as reported at the Washington Meeting of the American Physical Society, 1955 [Page, Heinberg, Wallace, and Trout, Phys. Rev. 99, 665(A) (1955)], some doubt had been felt as to the staying qualities of the quenching effect in fused quartz which has now been dispelled. Incidentally, a violet coloring grows gradually after several weeks close exposure to the Na<sup>22</sup> source; however, the quenching effect becomes apparent immediately when an unused fused quartz sample is inserted in the apparatus—based on two samples obtained. Crystalline quartz samples remain clear.

Narrowness,  $\nu$ , for aluminum was run with exactly the same procedure as for fused quartz. The result was  $1.182 \pm 0.011$ ,  $1.217 \pm 0.012$ , for 16.3 kilogauss and zero field, respectively. The discrepancy (probably not significant) is seen to be in the opposite direction to the quenching effect in fused quartz and Teflon. For crystalline quartz also,  $\nu$  was measured at 16.3 kilogauss and at zero field, using the three angles,  $\theta=0$  and  $\pm 4.2$  milliradians for the determination. The respective  $\nu$  values were  $0.719 \pm 0.012$  and  $0.718 \pm 0.011$ .

Extensive quenching data were taken with a polyethylene sample, chosen for its low atomic number and density, and its narrowness.

At this point in the experimental operations, the defining pad to the left of the sample in Fig. 8(a) was replaced by a mercury pool, Fig. 8(b), the level of which can be raised or lowered by means of lucite plungers running on screws. It is thus possible to scan the sample (in an integral fashion, since there is no continuously movable upper defining jaw) from the flat surface where the positrons enter, to beyond the greatest depth of penetration of the positrons. The calculated attenuation through the mercury pool is  $4 \times 10^3$  for 0.51-Mev gammas; so, for mercury settings giving

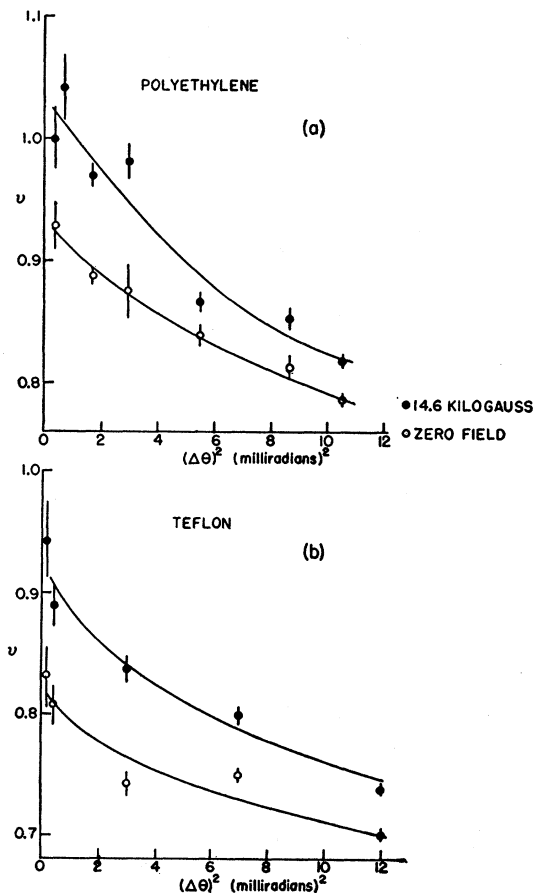


FIG. 11. Narrowness,  $\nu$ , as a function of  $(\Delta\theta)^2$  for (a) polyethylene, (b) Teflon.

attenuation in coincidence rate greater than  $\sim 10^2$ , the mercury absorber was supplemented by a lead brick (not shown) before proceeding deeper into the sample.

It was thought a worthwhile check on the apparatus, and on the quenching process itself, to measure narrowness  $\nu$ , as a function of depth in the sample. Accordingly, the data of Fig. 10 were taken, with  $\Delta\theta = 1.3$  milliradians; the three angles used were  $\theta = 0, \pm 3.3$  milliradians. For each setting of the mercury pool, the upper jaw of the defining slit system on the left of Fig. 8(a) was adjusted vertically by shims so that the maximum sample width seen by detector *A* was very nearly one-half of the detector slit width.<sup>20</sup>

From Fig. 10, it is seen that  $\nu$  as measured including the surface of the polyethylene sample is not significantly different from that measured excluding the surface. Time did not permit good counting statistics to accumulate for the rather deep (70 mg/cm<sup>2</sup>) setting. However, it is felt that the alignment is such that the runs at 18 and 31 mg/cm<sup>2</sup> depth contain no surface counts. Thus the quenching effect is not confined to the surface.

It was thought advisable to look for optimum resolution (the coincidence rate goes as the square of  $\Delta\theta$ ) at which to run quenching tests in future experiments, and also to get some idea of the ultimate width of the narrow component and of the magnetically enhanced portion of it. Measurement was made of the narrowness,  $\nu$ , at 14.6 kilogauss and at zero field, as a function of  $\Delta\theta$ , always keeping the effective width of the sample at one-half the width of the detector slits. These data are shown in Fig. 11(a). The points have been corrected for background. Peak-to-background was at least 200:1 for all points except those at less than one milliradian where it was 70:1 to 120:1, being the same for field on as for field off. The zero field curve apparently does not become flat as  $(\Delta\theta)^2$  goes to zero.

Teflon was tested in the same manner, using the same three angles,  $\theta = 0, \pm 3.3$  milliradians to determine  $\nu$ . The resulting curves of  $\nu$  versus  $(\Delta\theta)^2$  are shown in Fig. 11(b).  $\nu$  was also determined for Teflon at these field settings, with  $\Delta\theta = 1.7$  milliradians but using the three angles,  $\theta = 0, \pm 5$  milliradians. The results for field on and for field off were  $1.235 \pm 0.019$  and  $1.064 \pm 0.017$ .

From Fig. 11, it is concluded that it would not be profitable to run with the slits much narrower than one or two milliradians, in any *long-term* experiment to make, say, a careful field-dependence measurement of quenching.

Polyethylene data were taken in a manner quite similar to that earlier for Teflon [refer to Fig. 9(a) and (b)] and is shown in Figs. 12(a) and 12(b). The fraction of two-quantum annihilation events transferred

<sup>20</sup> The coincidence rate versus depth, *z*, in the sample is so closely of the form  $\exp(-kz)$  that this precaution seems hardly necessary, but is easily taken using the coincidence rate as indicator, with detector slit *B* opened wide.

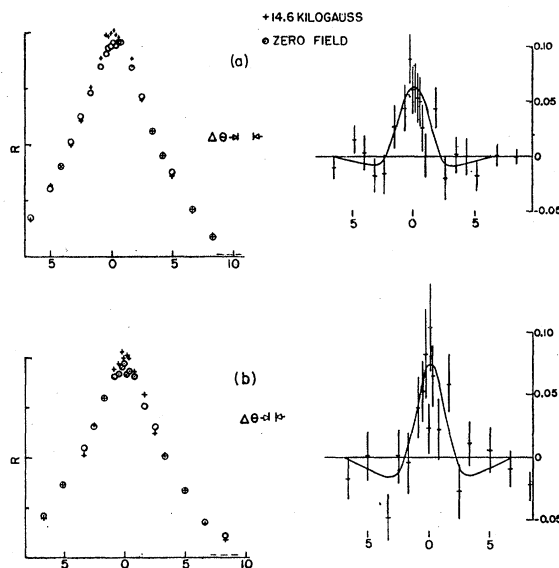


FIG. 12. Polyethylene quenching at two resolutions: (a)  $\Delta\theta = 1.2$  milliradians, (b)  $\Delta\theta = 0.6$  milliradian. Abscissas are  $\theta$  in milliradians. Difference data, field on minus field off, expressed as fractions of the peak rate, are shown at the right.

to the narrow component, estimated as 2.7%, is here significantly less than for Teflon, and its width (admittedly run with narrower  $\Delta\theta$ , and with more careful gamma ray definition at the sample) is somewhat narrower. It turned out that  $\nu$  for zero field was consistent with  $\nu$  inferred from the earlier zero-field data (of Fig. 3) taken with the original source-sample assembly of Fig. 1(b).

It should be mentioned that a magnesium sample was inserted just prior to taking the above Teflon data and its  $\nu$  determined (with  $\Delta\theta = 1.3$  milliradians), at 14.6 kilogauss and at zero field. Coincidence rate was measured at the peak and at  $\theta = \pm 3.3$  milliradians. The values for field on and for field off were  $0.767 \pm 0.007$  and  $0.768 \pm 0.007$ .

From the magnetic quenching results to date, it seems quite probable that any material having no  $\tau_2$  component, and likewise no narrow component as judged from the curve shape, will show no change in angular correlation when a strong field is applied. On the other hand, for those materials known to have a  $\tau_2$  component, and likewise a narrow component, it is generally possible to divert up to several percent of the total two-quantum events into the narrow component.

#### (4) Search for Diffusion of Annihilation Centers

By an "annihilation center" is meant the point in space from which the two quanta come. It was mentioned in subsection (3), during the discussion of polyethylene, that a mercury pool had been installed immediately to the left of the sample, whose purpose was to mask off (so far as detector *A* is concerned, see

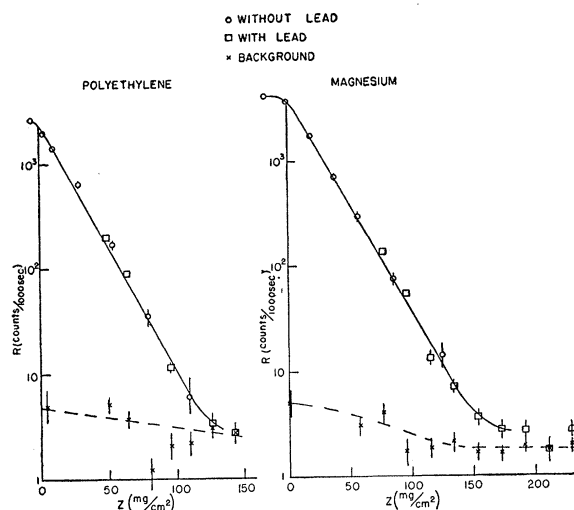


FIG. 13. Coincidence rate at the peak of the angular correlation, as a function of the height of mercury in the pool expressed in  $\text{mg}/\text{cm}^2$  of the sample. Points have not been corrected for background which is plotted separately as crosses.

Fig. 1) gammas coming from less than a given depth in the sample.

It was thought worthwhile to survey a few materials in the following manner: Detector  $A$  was set for  $\Delta\theta = 2.1$  milliradians; detector  $B$  was opened to its full  $\Delta\theta$  of 5 milliradians in the interest of counting rate. The left-hand upper defining jaw [refer to Fig. 8(a)] was set abnormally high so as not to interfere with gammas originating deep in the sample. Coincidence rate was then measured at the peak of the angular correlation as a function of height of the mercury level and typical results are shown in Fig. 13. For a given sample, many sweeps were made with the mercury, and no difficulties were encountered in resetting the mercury. Counter  $B$  was moved very slightly, in sympathy with the mercury level, so that it remained at the angular correlation peak.

Figure 13 shows data for polyethylene and magnesium, the lightest plastic material and the lightest metal run (the circles are data with only the mercury pool as absorber, the squares are data with an auxiliary lead brick backing up the mercury absorber). It happens that the logarithm of the coincidence rate,  $R$ , versus depth in the sample,  $z$ , is quite linear over about two decades, for all materials run. The characteristic slopes for the two materials shown here are in about the same ratio (within 3%) as the respective electron densities which is to be expected. No correction has been made for background, and it (taken to be coincidence rate with  $\theta$  displaced upwards 19 milliradians from the peak) is plotted separately in the figure. Lucite, Teflon, crystalline and fused quartz, aluminum, copper, and iron have been surveyed in this manner. The characteristic slopes of the linear portions are found to go approximately as the density, over this range of 8 in density. With a 15-kilogauss

field on, an excess rate (about 5%) appears at and to the left of the knee, and gradually dwindles with depth, being gone at perhaps one decade attenuation. The excess coincidence rate at the knee was down to about 2% when the source-sample distance was smaller (see for example the Teflon data of Fig. 9). This is not simply a result of the enhanced narrow component (when it exists) but was found to involve the angular distribution as a whole. It is interpreted as the focusing effect already discussed in Sec. II (3) and reference 17.

There is no evidence at present of diffusion of annihilation centers beyond the extrapolated range of the position spectrum either in narrow-component materials or metals or an insulating crystal. However, for a more definite answer to this question, it is planned to make careful runs deep in the sample, with field on and field off.

### III. DISCUSSION

Materials shown by Bell and Graham to exhibit a complex decay scheme for positrons have been shown here to exhibit a pointed angular correlation of the annihilation quanta, while those having a simple decay scheme have a blunt angular correlation. This connection between the presence of a  $\tau_2$  component in the decay with a narrow component in the angular correlation suggests that the two arise from a common source. It may be that the narrow component has a mean life  $\tau_2$ , but no verification of this is known, or it may be that the conditions favorable to the formation of a  $\tau_2$  component also are favorable to a narrow component partly or completely in parallel with the  $\tau_2$  component. In any event, these two anomalies seem always to occur together.

For materials having a pointed angular correlation, and a  $\tau_2$  component, an enhancement of the amount of the narrow component by means of a magnetic field has been demonstrated. Assuming the long lifetime  $\tau_2$  to be due to formation of  $^3S$  states of "positronium," this enhancement is regarded as a manifestation of magnetic quenching of such states.<sup>21</sup> To use fused quartz as an example, comparing the estimated fraction of narrow component, 0.18, with the fraction of long-lived component, 0.29, one concludes that  $\sim 0.4$  of  $\tau_2$  should be available for transfer into the narrow component by means of an applied magnetic field. If there is parallel formation of narrow component (presumably singlet states) this estimate should be

<sup>21</sup> A companion effect, the verification of which is not known, would be the decrease in the mean lifetime  $\tau_2$  due to the introduction of an alternative mode of decay. *Note added in proof.*—As reported at the International Conference on Quantum Interactions of the Free Electron, University of Maryland, April, 1956, M. Deutsch finds the detailed distribution in delay time for Teflon in part shortened by a strong magnetic field and in part unaffected, implying essentially no transitions between the three triplet states; V. Telegdi reports the magnetic sensitivity of the three-quantum yields from Teflon and fused quartz to be consistent with quenching of the  $m=0$  fraction of the triplet states in competition with the respective Bell and Graham decay rates for  $\tau_2$ .



raised. The observed fractional transfer into the narrow component at  $\sim 15$  kilogauss, namely 0.03 in polyethylene, 0.04 in Teflon (and a like figure for fused quartz), is about what one would calculate on the basis of the known values of  $\tau_2$  and the singlet-triplet energy difference for free 1-S positronium, assuming, for the sake of argument, that one-third of 0.29 of the total annihilation events are transferable.

Current experiments designed to measure the narrowness  $\nu$  [defined in Sec. II (3)] as a function of magnetic field, with temperature as a parameter, are expected to yield information on positron-electron overlap and/or whether more than one-third (the  $m=0$  fraction) of the supposed triplet states are available for quenching.

All that can be said about the diffusion experiments at this time has been stated in Sec. II (4).

An experiment under way is to test for narrow component enhancement in gases known to form

positronium, since free and thermalized positronium should yield a rather narrow correlation in contrast to bound positronium. Here again, the field dependence of any effect should be of interest.

It would seem worthwhile to look for a Doppler-free component in the energy spectrum<sup>22</sup> of the annihilation photons. Plans have been made for a nuclear resonance fluorescence experiment.

#### IV. ACKNOWLEDGMENTS

The authors are grateful to A. J. Allen for his support, and acknowledge the assistance of O. J. Wallace and T. W. Trout in the earlier stages of the work. Also assisting, but more recently, are D. Conway, R. Gunst, A. McElroy, and C. Richardson. For fabrication of mechanical parts we are indebted to E. M. Perkins and W. L. Cook. P. Stehle is to be thanked for his interest throughout the experiment.

<sup>22</sup> DuMond, Lind, and Watson, *Phys. Rev.* **75**, 1226 (1949).

## Application of the Rayleigh-Schrödinger Perturbation Theory to the Hydrogen Atom

RICHARD E. TREES\*

*Palmer Physical Laboratory, Princeton University, Princeton, New Jersey*

(Received March 6, 1956)

Wigner has calculated the ground-state energy of the hydrogen atom with second-order perturbation theory, the whole electrostatic potential being considered as the perturbation. Though his result is finite, it does not agree with the known energy for hydrogen. A fact implicit in the literature, but not usually appreciated in this connection, is pointed out—that if part of the electrostatic energy is retained in the zero-order problem, a correct result is obtained, even if the part of the energy retained is given a zero magnitude after the calculation is carried out. It is also shown that if the calculation is carried out in an Einstein hypersphere, the entire “electrostatic potential” can be regarded as the perturbation and the correct result is obtained. Perturbation theory leads to the exact energy eigenvalue in all approximations higher than the first, but the expansion of the eigenfunction converges slowly if the perturbation is made large.

### I. INTRODUCTION

WIGNER<sup>1</sup> has recently pointed out a failure of second-order perturbation theory to give a meaningful result when applied to the hydrogen atom. Considering the whole electrostatic potential as a perturbation, he has calculated the ground-state energy and found it finite, but grossly incorrect numerically. It would be very simple to carry out perturbation calculations if the solutions of the field-free Schrödinger equation could be used as a starting point, but the results of I show that this cannot be done. The present investigation is part of an effort to find a modification that will give the correct result without introducing too much additional complication.

In the type of problem considered, the exact solution

of the Schrödinger equation is assumed already known, or at least obtained to a high degree of accuracy with variational methods. In the simplest case, the Hamiltonian depends linearly on a single parameter  $\lambda$  which has a continuous range of values. The energy eigenvalue of the Hamiltonian  $H(\lambda)$  will be some known function  $E(\lambda)$ . The parameter  $\lambda$  is then regarded as a sum of two parameters, say  $\lambda = \lambda_1 + \lambda_2$ . The eigenfunctions and eigenvalues of  $H(\lambda)$  are then obtained with perturbation theory,<sup>2</sup> starting from zero-order solutions of  $H(\lambda_1)$ . This procedure defines the energy as a series in increasing powers of  $\lambda_2$ . If the correct energy,  $E(\lambda) = E(\lambda_1 + \lambda_2)$ , has an expansion in increasing powers of  $\lambda_2$  that agrees with the perturbation series to a given order, then the energy calculated with the perturbation theory is considered correct to that order. Usually perturbation theory can be correct only when  $\lambda_2 < \lambda_1$ , as

\* On leave from the National Bureau of Standards, Washington, D. C.

<sup>1</sup> E. P. Wigner, *Phys. Rev.* **94**, 77 (1954); referred to as I in this paper.

<sup>2</sup> E. U. Condon and G. H. Shortley, *The Theory of Atomic Spectra* (Cambridge University Press, London, 1935).